

# Formulation of nanotized curcumin and demonstration of its antimalarial efficacy

Aparajita Ghosh<sup>1</sup>  
Tanushree Banerjee<sup>2</sup>  
Suman Bhandary<sup>1</sup>  
Avadhesha Surolia<sup>3</sup>

<sup>1</sup>Division of Molecular Medicine, Bose Institute, Centenary Campus, Kolkata, West Bengal, India; <sup>2</sup>Department of Biotechnology, University of Pune, Pune, India; <sup>3</sup>Molecular Biophysics Unit, Indian Institute of Science, Bangalore, India

**Aim:** The present study was conducted to overcome the disadvantages associated with the poor water solubility and low bioavailability of curcumin by synthesizing nanotized curcumin and demonstrating its efficacy in treating malaria.

**Materials and methods:** Nanotized curcumin was prepared by a modified emulsion-diffusion-evaporation method and was characterized by means of transmission electron microscopy, atomic force microscopy, dynamic light scattering, Zetasizer, Fourier transform infrared spectroscopy, and differential thermal analysis. The novelty of the prepared nanoformulation lies in the fact that it was devoid of any polymeric matrices used in conventional carriers. The antimalarial efficacy of the prepared nanotized curcumin was then checked both in vitro and in vivo.

**Results:** The nanopreparation was found to be non-toxic and had a particle size distribution of 20–50 nm along with improved aqueous dispersibility and an entrapment efficiency of 45%. Nanotized curcumin (half maximal inhibitory concentration [IC<sub>50</sub>]: 0.5 μM) was also found to be ten-fold more effective for growth inhibition of *Plasmodium falciparum* in vitro as compared to its native counterpart (IC<sub>50</sub>: 5 μM). Oral bioavailability of nanotized curcumin was found to be superior to that of its native counterpart. Moreover, when *Plasmodium berghei*-infected mice were orally treated with nanotized curcumin, it prolonged their survival by more than 2 months with complete clearance of parasites in comparison to the untreated animals, which survived for 8 days only.

**Conclusion:** Nanotized curcumin holds a considerable promise in therapeutics as demonstrated here for treating malaria as a test system.

**Keywords:** curcumin, nanotized curcumin, *P. berghei*, *P. falciparum*, antimalarial

## Introduction

In traditional Indian medicine (Ayurveda), the natural product curcumin (1,7-bis(4-hydroxy 3-methoxy phenyl)-1,6-heptadiene-3,5-dione) which is a polyphenolic compound extracted from the rhizome of *Curcuma longa L.* (family Zingiberaceae) along with other curcuminoids, has been considered as an efficacious molecule for the treatment of various disorders. Recent studies have substantiated and provided scientific evidence regarding its prophylactic and therapeutic potential, unravelling its antiinflammatory, anticarcinogenic, and antiinfectious activities.<sup>1–3</sup> The cytotoxic and parasiticidal effects of curcumin have been demonstrated against protozoan parasites such as *Leishmania*, *Trypanosoma*, *Giardia*, and *Plasmodium falciparum*.<sup>4–7</sup> Curcumin displayed inhibitory activity against a *Plasmodium berghei*-infected model of malaria in mice, and was found to be synergistic with artemisinin.<sup>8,9</sup> However, curcumin has a number of inherent drawbacks such as poor absorption and low serum and tissue levels, and hence low bioavailability (BA).<sup>10</sup>

To overcome these shortcomings, many novel approaches such as the development of polymeric and lipidic nanoparticles, etc, have already been explored to improve its pharmacokinetic profile.<sup>11,12</sup> The small size of these systems provides longer circulation duration to

Correspondence: Avadhesha Surolia  
Molecular Biophysics Unit, Indian Institute of Science, Bangalore 560 012, India  
Tel +91 80 22932389, 22932714  
Fax +91 80 23600535  
Email surolia@mbu.iisc.ernet.in

the encapsulated drugs, leading to enhanced organ penetration and retention.<sup>13,14</sup> However, the safety of most of the nanocarriers and their biocompatibility still remains unresolved.<sup>13</sup>

To surmount these disadvantages, in the present work, we used chemically synthesized pure curcumin to develop nanotized curcumin, the size of which was reduced to 20–50 nm, in diameter, by a modified emulsion-diffusion-evaporation method. The therapeutic effectiveness of the formulation depends on the enhanced availability of the drug at the site of action, which again depends on adequate aqueous solubility of the drug leading to improved BA. The solubility of a drug is often fundamentally related to drug particle size. As a particle decreases in size, the surface area increases. This larger surface area therefore allows greater interaction with the solvent, which results in increased dispersibility and solubility. In the present study, the aim of formulating nanotized curcumin was to enhance the BA of curcumin, which has always remained a challenge in the past. The efficacy of the nanotized formulation was tested in the inhibition of *in vitro* *P. falciparum* culture growth<sup>15</sup> and *in vivo* cerebral malaria mice model, viz, *P. berghei*-infected mice.<sup>16</sup> The nanopreparation was devoid of polymeric matrices used in conventional carriers and hence free of their potential side effects as well. Also, it was freely and uniformly dispersible in water. The nanotization of curcumin described here is easily scalable and therefore represents an advancement in comparison to conventionally used nanocarriers and is suitable for treating not only malaria, used here as a test system, but may also have a potential application in other therapeutic areas.

## Materials and methods

### Materials

Roswell Park Memorial Institute 1640 medium and Albumax were obtained from Invitrogen BioServices India Pvt. Ltd., (Whitefield, Bangalore, India). Culture-grade glucose was acquired from HiMedia, Mumbai, India and the rest of the chemicals used were purchased from Sigma-Aldrich Co., (St Louis, MO, USA). *P. falciparum* was obtained from Dr Namita Surolia (Jawaharlal Nehru Centre for Advanced Scientific Research, Bangalore, India) and *P. berghei* was obtained from Dr R Juyal (National Institute of Immunology, New Delhi, India). Human fibroblast (L-929) was obtained from Sigma-Aldrich.

### Methods

#### Synthesis of curcumin

The isolation of natural curcumin from *C. longa* rhizome is a cumbersome and costly process. No practical methods have so far been found for an effective separation of curcumin from

two related compounds (methoxy and demethoxy curcumin) with which it is found in nature. This difficulty of separation has led to several efforts to synthesize the compound. For this study, pure curcumin was synthesized according to the method of Pabon<sup>17</sup> that involves condensation of vanillin and 2,4 pentanedione, followed by purification by crystallization from ethyl acetate/MeOH at 4°C (97% pure by high-performance liquid chromatography [HPLC] analysis; high resolution mass spectrometry calculated for C<sub>21</sub>H<sub>20</sub>O<sub>6</sub>H 369.1333, found 369.1324).

#### Preparation of nanotized curcumin

A modified emulsion-diffusion-evaporation method<sup>18,19</sup> was used to formulate the nanotized curcumin. In brief, 50 mg of the synthesized pure curcumin was dissolved in 5 mL of ethyl acetate at room temperature. The organic solution was then emulsified with an aqueous phase containing didodecyltrimethylammonium bromide (DMAB). The resulting oil-in-water emulsion was stirred at room temperature for 3 hours before homogenizing at 15,000 rpm for 5 minutes with a high-speed homogenizer (Polytron PT4000; Polytron Kinematica, Lucerne, Switzerland). Subsequently, the organic solvent was removed by rotary evaporation and the aqueous phase containing the drug was sonicated for 30 minutes. The resulting aqueous emulsion was centrifuged at 35,000 rpm for 1 hour and the nanoprecipitate was suspended in phosphate buffered saline (PBS), along with sucrose and glucose (used as a cryoprotectant) added at a concentration of 20%, lyophilized, and stored at room temperature for future use. The lyophilized preparation of nanotized curcumin thus prepared was found to be devoid of ethyl acetate and DMAB.

#### Dynamic light scattering studies of nanotized curcumin

The particle diameter of curcumin nanoparticles was measured by dynamic light scattering (DLS) performed on a Malvern Zetasizer S90 series (Malvern Instruments, Malvern, UK). The sample was prepared by taking 1 mg of the lyophilized nanotized curcumin powder in 10 mL of distilled water.

#### Zeta potential measurements of nanotized curcumin

The stability of the curcumin nanoparticles was determined by zeta potential measurements using a Malvern Zetasizer Nano ZS (Malvern Instruments). Prior to analysis, the solutions were filtered through a 2 µm filter. Each sample was measured in triplicate.

#### Transmission electron microscopy studies of nanotized curcumin

The transmission electron microscopy (TEM) observations were performed with a TECNAI G2 BIOTWIN system at

a magnification of 9.9×. Initially, 10 µL of the nanotized curcumin suspension was retrieved and placed upon 300-mesh carbon-coated copper grids. The grids containing the samples were dried extensively under a lamp. The grids were then stained with 2% phosphotungstic acid solution followed by vigorous washing with a thin flow of Milli-Q water. The stained grids were then dried, inserted in the sample receiver, and allowed to wait until the machine created a vacuum before obtaining images. The images of the samples were captured and the particle diameter was measured using SIS software at different magnifications.<sup>20</sup>

### Atomic force microscopy studies of nanotized curcumin

The atomic force microscopy (AFM) was performed with a picoview AFM system (v1.10.4; Agilent Technologies, Santa Clara, CA, USA). All the images were obtained in the acoustic mode using cantilevers having a resonance frequency of 146–236 kHz, tip height of 10–15 µm, and tip length of 225 µm. Mica was chosen as a solid substrate and used immediately after cleavage in a clean atmosphere. During the characterization experiment, the probe and cantilever were immersed completely in the water solution. The nanotized suspensions on mica were dried in air (65% humidity) for 30 minutes. Images were analyzed with the help of Pico Image Software from Agilent Technologies.<sup>21</sup>

### Fourier transform infrared spectroscopy studies of nanotized curcumin

Fourier transform infrared (FT-IR) spectroscopy of native curcumin and nanotized curcumin was performed on a FT-IR spectrophotometer (Spectrum 100 optica; PerkinElmer Inc., Waltham, MA, USA). The pellets of sample (10 mg) and potassium bromide (200 mg) were prepared by compressing the powders at 5 bars for 5 minutes on a KBr press and the spectra were scanned on the wavenumber range of 4,000–450 cm<sup>-1</sup>.

### Differential thermal analysis

The relative states of DMAB, native curcumin, and nanotized curcumin with respect to the change in temperature were studied using a thermal analyzer (STA 449 F3 Jupiter; NETZSCH, Selb, Germany). Lyophilized DMAB powder (5–10 mg), native curcumin, and nanotized curcumin were placed in a platinum pan and heated from 30°C to 300°C at a heat flow rate of 5°C/minute, under a constant flow (100 mL/minute) of nitrogen gas.

### Determination of drug loading and entrapment efficiency

The amount of curcumin loading and its entrapment efficiency was measured by dissolving the pellet of nanotized curcumin in 2 mL of ethyl acetate for 3 days at 4°C. The amount of the curcumin in solution, thus released, was measured by its absorbance at 430 nm with respect to a standard curve of curcumin solution in ethyl acetate. The percentage entrapment was calculated using the following equation:

$$\text{Loading efficiency \%} = \frac{\text{Weight of nanotized curcumin}}{\text{Weight of nanoparticles}} \times 100.$$

$$\% \text{ Entrapment efficiency} = \frac{\text{Amount of curcumin practically present in the nanotized curcumin}}{\text{Amount of curcumin theoretically present in the nanotized curcumin}} \times 100$$

### In vitro release kinetics of nanotized curcumin

A known amount of lyophilized nanotized curcumin was dispersed (2 mg) in 10 mL phosphate buffer (pH 7.4) and the solution was divided equally into ten microfuge tubes (1 mL each). The tubes were kept in a thermostable water bath set at room temperature. Free curcumin is known to be completely insoluble in water. Therefore, at predetermined intervals of time, the solution was centrifuged at 3,000 rpm for 10 minutes to pelletize the released drug (curcumin), leaving the nanotized curcumin in the supernatant. The pellets were dissolved in ethanol and the amount of curcumin released was quantified spectrophotometrically at a wavelength of 430 nm.

### Analysis of photophysical properties of native curcumin and nanotized curcumin

To determine whether nanotization had any effect on curcumin's photophysical properties, spectroscopic analysis was conducted.<sup>22</sup> The fluorescence emission spectra of both native curcumin and nanotized curcumin were recorded in a fluorescence spectrophotometer (F-7000; Hitachi Ltd., Tokyo, Japan) from 450 nm to 650 nm with an excitation wavelength of 420 nm.

### Cell viability assay

The cell viability assay was conducted by the methyl thiazol tetrazolium bromide (MTT) assay using MTT reagent (Sigma-Aldrich) as described in a previous study.<sup>23</sup> Human fibroblast L-929 cells were plated in a 96-well microtiter plate at a

density of  $1 \times 10^4$  cells per well in a final volume of 100  $\mu\text{L}$  Dulbecco's Modified Eagle's Medium. The cells were treated with different concentrations of native and nanotized curcumin (8.11, 16.23, 32.47, 64.94, and 129.88  $\mu\text{mol/L}$ ) for 24, 48, and 72 hours. After treatment, the cells were incubated with MTT solution (12 mM) for 2 hours at  $37^\circ\text{C}$ . The formazan crystals formed were dissolved in dimethyl sulfoxide at  $37^\circ\text{C}$  for 1 hour in the dark, and the absorbance was read at 595 nm in a microplate reader (Model 3,550; Bio-Rad Laboratories Inc., Hercules, CA, USA).

### Nanotized curcumin uptake assay

An uptake assay of nanotized curcumin was performed to assess the concentration of curcumin inside erythrocytes. Experiments were performed in the first and second cycle of parasite growth. Five flasks were taken as a) parasitized erythrocytes with no drug (control); b) parasitized erythrocytes treated with 1  $\mu\text{M}$  curcumin; c) parasitized erythrocytes treated with 1  $\mu\text{M}$  nanotized curcumin; d) uninfected erythrocytes treated with 1  $\mu\text{M}$  curcumin; and e) uninfected erythrocytes treated with 1  $\mu\text{M}$  nanotized curcumin. Control and treated flasks had equal parasitemia at the beginning of the experiment. Hematocrit in all the flasks was kept at 10%. Uptake assay by fluorimetry was performed as described in a previous study.<sup>24</sup> Fluorescence readings from control flasks were considered as background and readings from flasks containing treated and uninfected erythrocytes were normalized with respect to the background reading. A standard curve for the fluorescence of curcumin and nanotized curcumin was used to correlate the fluorescence intensity to determine the uptake of curcumin by the infected and uninfected erythrocytes.

### Determination of growth inhibition of blood-stage parasite by microscopy

To monitor the effects of nanotized curcumin on asexual stages of the parasites by microscopy, human red blood cells (RBCs) were infected with synchronized rings of *P. falciparum* 3D7 strain (chloroquine sensitive). The infected RBCs were cultured in 96-well plates at 10% hematocrit and 2% parasitemia. The medium was changed every 24 hours. Ten different concentrations of the formulation were used for checking its efficacy. All concentrations were tested in duplicate. Growth inhibition was monitored with standard Giemsa staining after 48 and 72 hours.<sup>25</sup> The percentage parasitemia was calculated from the ratio of infected RBCs to the total number of RBCs. RBCs were counted in at least ten different fields by using a light microscope. Dead parasites within the RBCs could be differentiated from the

live parasites by the absence of intact plasma membrane, shrunken size, and/or the absence of stained cytoplasm. Unhealthy parasites with vacuolar cytoplasm were not considered to be dead parasites.

### Evaluation of oral BA of nanotized curcumin

To directly investigate the oral BA of nanotized curcumin, pharmacokinetics analysis (Rutgers University protocol no: 99-015) was performed on C57BL/6 mice after oral administration with curcumin nanoemulsions. Mice were divided into two groups, each group consisting of six animals. One group of mice received native curcumin (20 mg/kg body weight) and the other group was given nanotized curcumin (20 mg/kg body weight) orally. Animals had access to water and food only after 4 hours of drug administration. Blood samples (0.2 mL) were collected into heparinized tubes, through the catheters which had been implanted into the right external jugular vein of mice at 0, 2, 5, 10, 15, 20, 25, and 30 hours after oral administration of curcumin. Normal saline (0.2 mL) was administered in order to compensate for the blood loss after collecting every blood sample. The plasma was separated from the heparinized blood, collected by centrifugation, and stored at  $-20^\circ\text{C}$  prior to HPLC analysis. All the mice used in this study received proper care in compliance with the Animal Ethics Committee, India (Registration no 38/99/CPC SEA).

The area under the curve (AUC) for the plot of the plasma concentration over time was evaluated using the linear trapezoidal method. The maximum concentration of curcumin ( $C_{\text{max}}$ ) and time at  $C_{\text{max}}$  ( $T_{\text{max}}$ ) were directly obtained from the curves. The elimination rate constant ( $K_{\text{el}}$ ) was calculated using the method of residuals, based on the oral absorption, one compartment model.

### Dose kinetics determination on C57BL/6 mice infected with *P. berghei*

C57BL/6 mice were infected with *P. berghei*-ANKA ( $2.5 \times 10^6$  parasites) intravenously. Post-infection, mice were given a biweekly oral treatment at three different doses, 10, 20, and 40 mg/kg body weight, of the native curcumin as well as its nanotized counterpart for 1 month. Parasitemia was calculated every fourth day. The optimum dose was determined by Peterson's test and mortality rate.<sup>26</sup>

### Evaluation of hepatoprotective and nephroprotective activity of nanotized curcumin

C57BL/6 mice were infected with *P. berghei*-ANKA ( $2.5 \times 10^6$  parasites) intravenously. Post-infection, mice were given a biweekly oral treatment with 20 mg/kg body weight



of the native curcumin as well as its nanotized counterpart for 1 month. After 1 month, blood samples were collected by puncturing the retro-orbital sinus. The blood was allowed to clot for 30 minutes. Serum was separated by centrifugation and was used for biochemical estimations.

## Results

### Characterization of nanotized curcumin

TEM analysis of the aqueous dispersion of nanotized curcumin showed that the particle size was in the range of 20–50 nm in diameter (Figure 1A), and AFM of the powdered sample showed the particles to be mostly around 50 nm in diameter (Figure 1B). The nanotized curcumin was dispersible in water unlike its native counterpart, which is only soluble in organic solvents such as dimethyl sulfoxide (Figure 1C). DLS of an aqueous dispersion of nanotized curcumin revealed the formation of nanoparticles with an average diameter of 20–50 nm (Figure 1D). Dry, lyophilized powder of nanotized curcumin was found to be stable, both physically and chemically, was readily dispersible in water, and could be stored at room temperature for almost 1 year without any decomposition or aggregation. The zeta potential is an important factor for understanding the state of the nanoparticle surface. It also predicts the long-term stability of the nanoparticles and is a significant factor in determining their interaction *in vivo* with the cell membrane. The zeta potential of nanotized curcumin was found to be  $63.2 \pm 6.96$  mV (Figure 1E), suggesting high stability of the formulation. FT-IR spectroscopy was performed to elucidate the structural similarity of native curcumin and nanotized curcumin, as shown in Figure 2A. In native curcumin, a broad absorption band at  $3,504\text{ cm}^{-1}$  was due to the phenolic O–H stretching vibration, and this band was observed at  $3,445\text{ cm}^{-1}$  in nanotized curcumin, most probably due to –OH vibrations of intermolecular-bonded OH groups. Additionally, the strong band at  $1,626\text{ cm}^{-1}$  in native curcumin had a predominantly mixed  $\nu$  (C=C) and  $\nu$  (C=O) character. In the case of nanotized curcumin, these molecular vibrations were found at  $1,624\text{ cm}^{-1}$ . Another strong band at  $1,601\text{ cm}^{-1}$  in native curcumin was attributed to the symmetric aromatic ring stretching vibrations  $\nu$  (C=C ring) and the same was observed at  $1,596\text{ cm}^{-1}$  for nanotized curcumin. The sharp  $1,506\text{ cm}^{-1}$  band was assigned to the  $\nu$  (C=O), while an enol C–O band was obtained at  $1,273\text{ cm}^{-1}$  and a benzoate trans –CH vibration at  $960\text{ cm}^{-1}$  in curcumin. These bands were observed at  $1,521\text{ cm}^{-1}$ ,  $1,277\text{ cm}^{-1}$ , and  $968\text{ cm}^{-1}$ , respectively, in nanotized curcumin, indicating that the nanotized form of curcumin is akin to its native counterpart (Figure 2A).

To see the physical state of curcumin within the nanotized curcumin, thermal analysis was performed. In this study, differential thermal analysis (DTA) was used to further investigate the state/phase of nanotized curcumin (Figure 2B). The DTA curve of DMAB showed four endothermic peaks located at  $70.4^\circ\text{C}$ ,  $80.2^\circ\text{C}$ ,  $171.5^\circ\text{C}$ , and  $215.6^\circ\text{C}$ , successively. The DTA thermogram of native curcumin showed a strong endothermic peak at  $177.5^\circ\text{C}$ , indicating the melting point of curcumin and its crystalline nature. However, for nanotized curcumin, there was only one prominent endothermic peak at  $72.4^\circ\text{C}$ . Peaks observed at  $70.4^\circ\text{C}$  and  $72.4^\circ\text{C}$  (Figure 2B) correspond with the main phase transition temperature ( $T_m$ ) of DMAB and nanotized curcumin, respectively. At  $T_m$ , the double hydrocarbon chains of DMAB were from the gel (or ordered) phase transformed into the liquid crystalline (or fluid) phase. The origin of peaks at  $80.2^\circ\text{C}$  (Figure 2B) is perhaps related to the change in the orderliness of the small head groups of DMAB. The peak at  $171.5^\circ\text{C}$  corresponds with the melting temperature of DMAB, at which the electrostatic interactions among the head groups of DMAB are destroyed. The first endothermic peak of nanotized curcumin was higher than that of DMAB, which is attributed to the orderliness associated with tethering DMAB to the nanoformulation.

The loading and encapsulation efficiencies of nanotized curcumin were calculated and found to be 4.25% and 45%, respectively. Release of curcumin from nanotized curcumin occurred in a controlled manner, with just 50% of the drug being released by 24 hours. Even after 48 hours, the nanotized curcumin retained nearly 10% of the drug, suggesting that curcumin was well-entrapped within the nanotized curcumin (Figure 3A).

Further spectroscopic studies were carried out to investigate the effect of nanotization on the photophysical properties of curcumin. The fluorescence spectra of both native curcumin and nanotized curcumin (from 450 nm to 650 nm) in methanol:water (50% volume per volume) at an excitation wavelength of 420 nm showed sharp emission peaks at 550 nm (Figure 3B). However, the observed change in the fluorescence intensity of native curcumin compared to nanotized curcumin (200 au [arbitrary units] vs 350 au) suggested protection of curcumin molecules within the nanotized formulation (Figure 3B).

### Growth inhibition of L-929 (human fibroblast) cells by nanotized curcumin in a concentration- and time-dependent manner

The growth inhibition by nanotized curcumin in L-929 cells was observed after incubation for 24, 48, and 72 hours. No significant

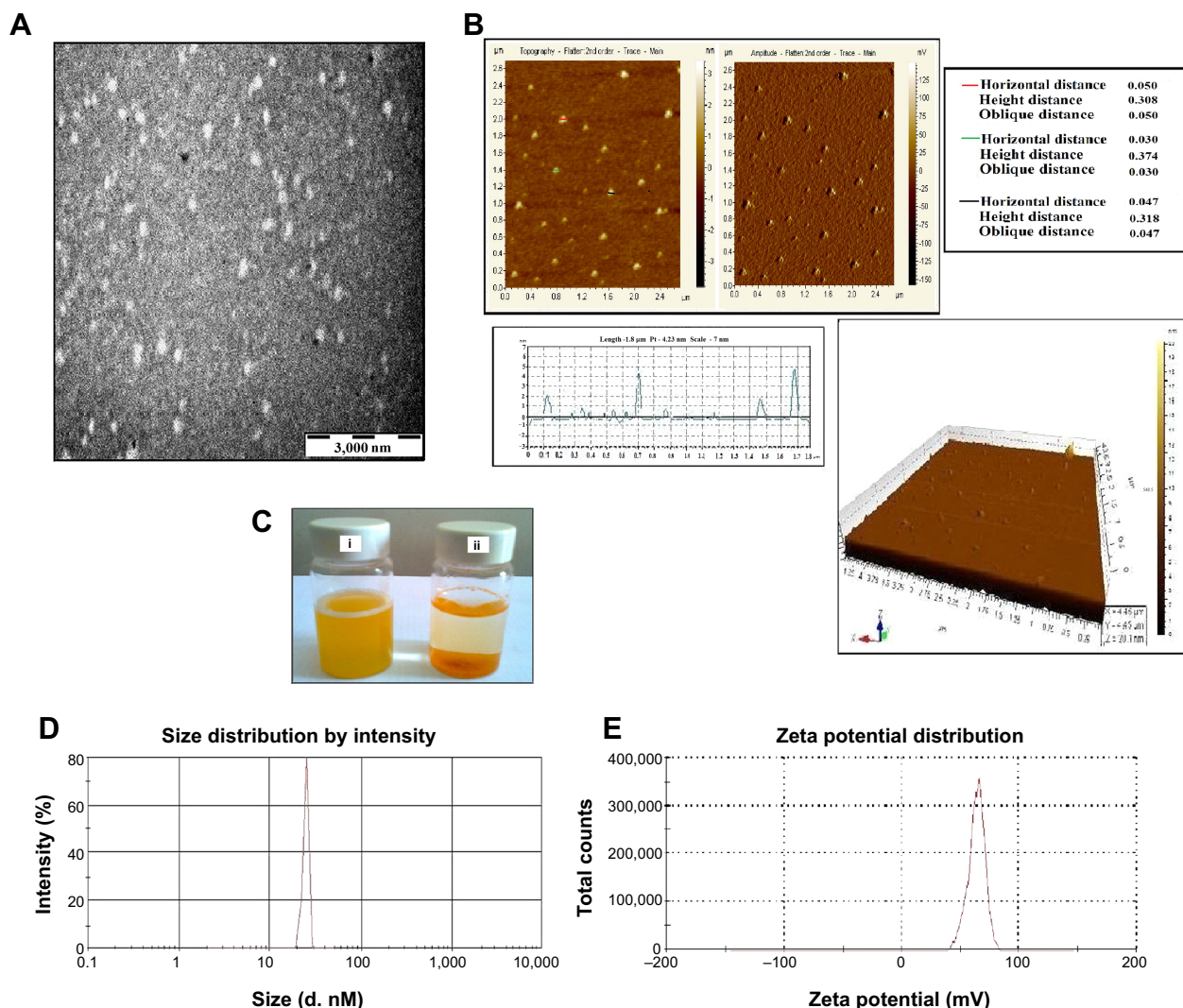


**Figure 1** (A) TEM pictures of nanotized curcumin at a magnification of  $9.9\times$  demonstrates particles with a spherical morphology and an average size distribution of 20–50 nm. (B) AFM images of nanocapsules obtained 2 minutes after deposition on mica support. Amplitude-flattened view of nanotized curcumin is shown. Horizontal cross section indicates the height of the nanocapsules from the substratum, ie, the mica sheet. (C) Dispersibility of (i) nanotized curcumin and (ii) native curcumin in water. (D) DLS-measured size distribution of nanotized curcumin; (E) zeta potential of nanotized curcumin.

**Abbreviations:** AFM, atomic force microscopy; DLS, dynamic light scattering; TEM, transmission electron microscopy; d, diameter.

cytotoxicity was observed in the cell lines treated with nanotized curcumin until 72 hours (Figure 4). Similarly, native curcumin also exhibited marginal cytotoxic effects on human fibroblasts (Figure 4). The resulting growth curves showed that the inhibition was both concentration- and time-dependent.

### Intraerythrocytic concentration of nanotized curcumin is much less than $1\ \mu\text{M}$

To test the uptake of nanotized curcumin within erythrocytes, the concentration of both native and nanotized curcumin in erythrocytes was measured after the first and second cycle of growth. In the first growth cycle, an average ( $n=3$ ) of 300 nM and 240 nM native curcumin were found inside the cells of

the treated cultures and uninfected erythrocytes, respectively (Figure 5A). Comparatively, 500 nM and 430 nM nanotized curcumin were found inside the cells of the treated cultures and uninfected erythrocytes, respectively (Figure 5A). In the second growth cycle, 250 nM and 100 nM native curcumin were found in the treated cultures and uninfected erythrocytes, respectively, while 400 nM and 270 nM nanotized curcumin were found in the treated cultures and uninfected erythrocytes, respectively. Hence, fluorometric estimation of curcumin uptake revealed that a smaller fraction of native curcumin as compared to the nanotized curcumin was taken up by the infected erythrocytes. This could be due to the increased uptake of nanotized curcumin into the erythrocytes, resulting in its increased intracellular concentration.

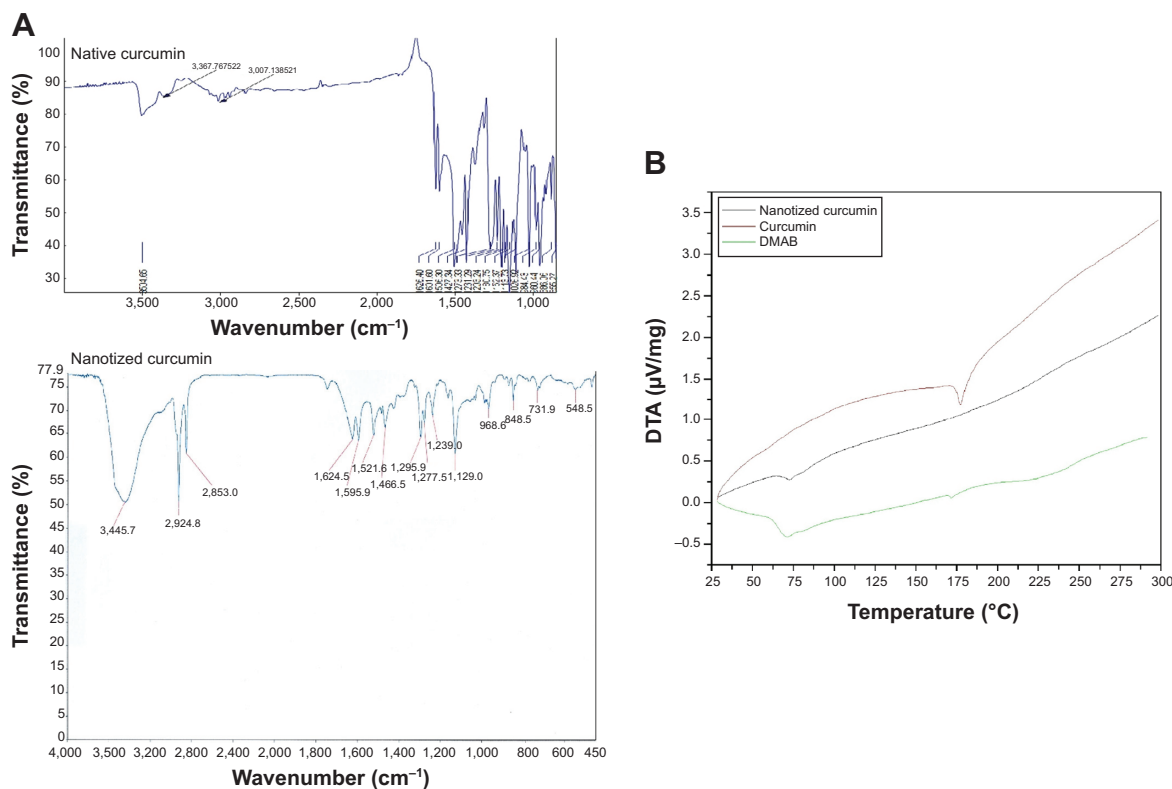


**Figure 2 (A)** FT-IR spectrum of native and nanotized curcumin. **(B)** DTA thermogram of native curcumin, nanotized curcumin, and DMAB.  
**Abbreviations:** DMAB, didodecyltrimethylammonium bromide; DTA, differential thermal analysis; FT-IR, Fourier transform infrared.

### In vitro inhibition of *P. falciparum* 3D7 blood-stage parasites

Curcumin and nanotized curcumin were checked for their antiparasitic activity against 3D7 (chloroquine-sensitive strain) in in vitro cultures. The half maximal inhibitory concentration ( $IC_{50}$ ) value for growth inhibition of parasites was found to be 5  $\mu$ M and 0.5  $\mu$ M, for native curcumin and

nanotized curcumin, respectively (Figure 5B). To find out the parasite stage in which these compounds act, a synchronized ring stage culture of *P. falciparum* was treated with a 2.5  $\mu$ M concentration of the native and nanotized forms of curcumin. Growth of the parasite was arrested at the trophozoite stage by both native curcumin and its nanotized form to varying extents. The parasites were completely eradicated and the

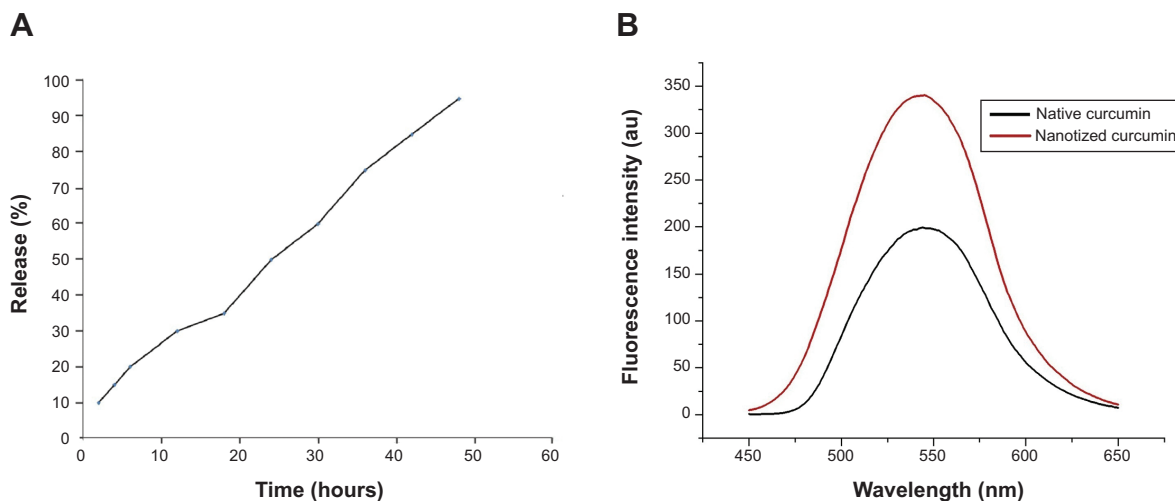


**Figure 3 (A)** Kinetic release of nanotized curcumin. **(B)** Fluorescence emission spectra of native and nanotized curcumin in an aqueous solution containing 50% methanol excited at 420 nm.

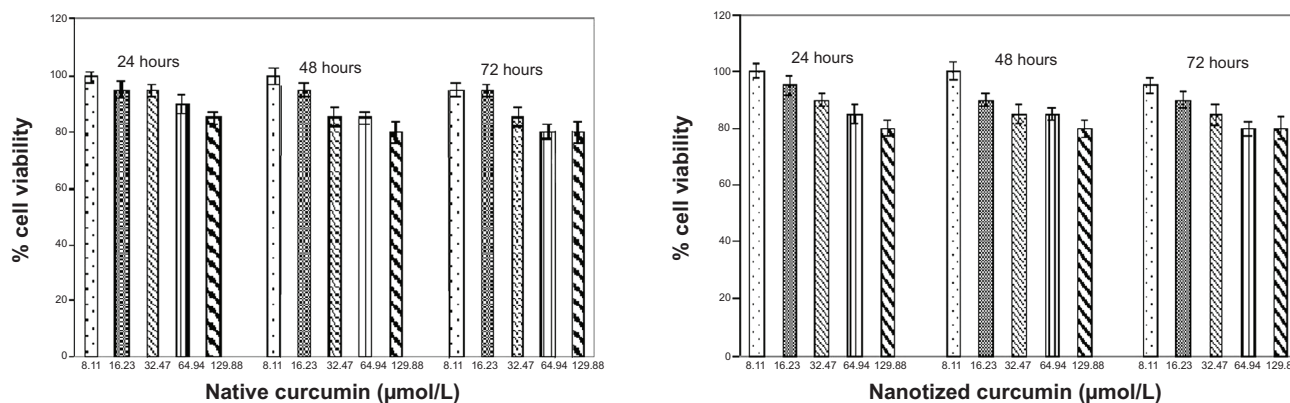


**Figure 4** Toxicity profile of nanotized curcumin. Human fibroblast (L-929) cells were exposed to different concentrations of native and nanotized curcumin (8.11, 16.23, 32.47, 64.94, and 129.88 μmol/L) for 24, 48, and 72 hours.

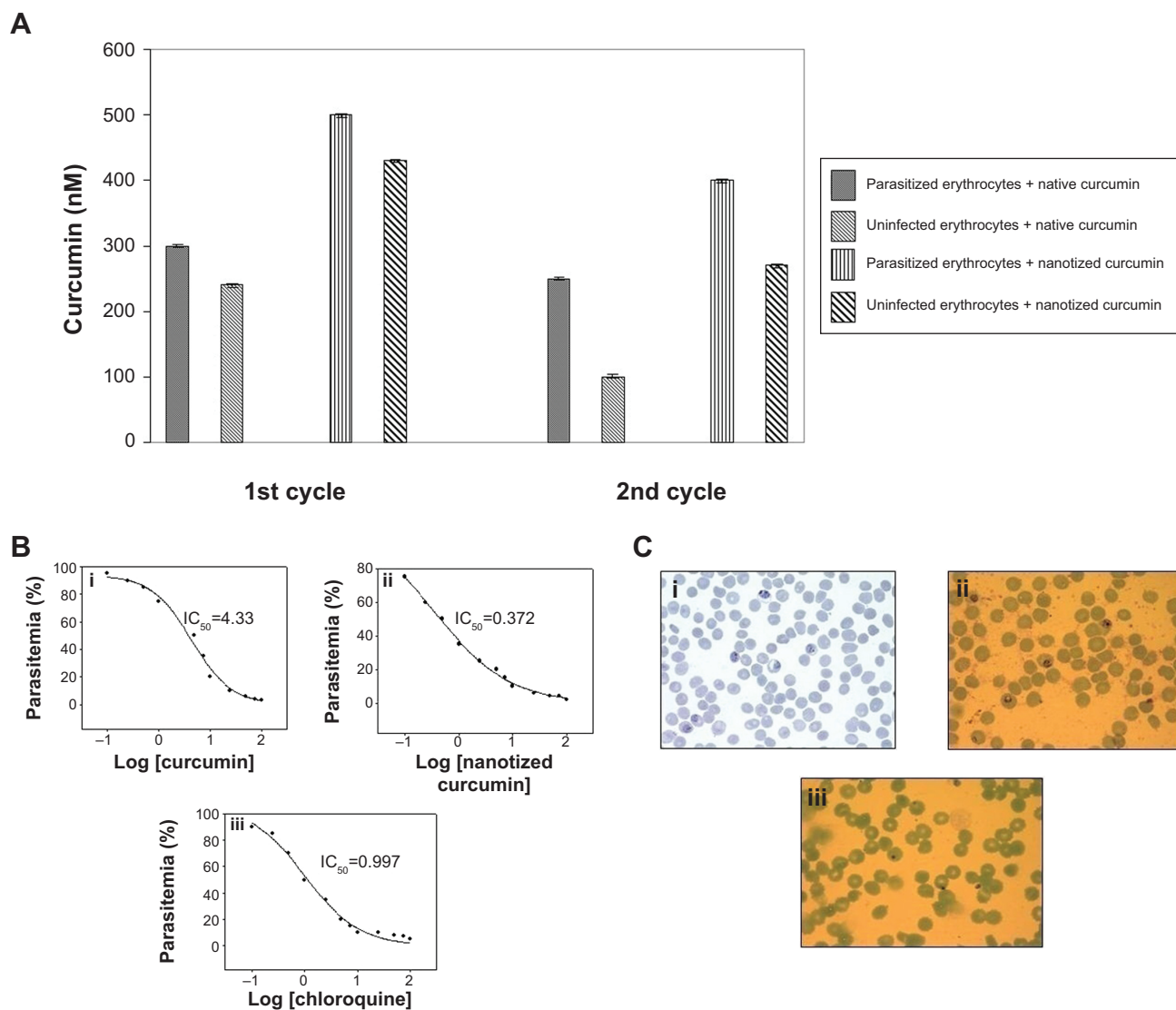


**Figure 5** (A) Curcumin uptake by parasitized and uninfected erythrocytes during first and second cycle of *Plasmodium falciparum* growth. (B) Inhibition of *P. falciparum* blood-stage of infection at a concentration of 0.5 μM after 72 hours of treatment with (i) native curcumin and (ii) nanotized curcumin. (iii) Chloroquine was used as the control drug. (C) Inhibition of *P. falciparum* blood-stage of infection at various concentrations of (i) native curcumin and (ii) nanotized curcumin. (iii) Chloroquine was used as the control drug.

**Note:** Error bars represent standard error of the mean (n=6).

**Abbreviation:** IC<sub>50</sub>, half maximal inhibitory concentration.



RBCs appeared to be devoid of the parasites upon treatment with nanotized curcumin for 72 hours (Figure 5C). On the other hand, only 60% of the parasites were eradicated upon treatment with native curcumin (Figure 5C).

## Nanotized curcumin was more bioavailable than native curcumin

To find out the oral BA of curcumin in its native and nanotized forms, pharmacokinetics analysis was performed on mice after oral administration with native or nanotized curcumin (40 mg/kg body weight). No curcumin was detected above the limit of detection from the plasma of the mice treated with native curcumin. All of the plasma samples were therefore incubated with glucuronidase and sulfatase to convert the major curcumin metabolites, curcumin glucuronide and sulfate, back to curcumin before HPLC quantification. As shown in Figure 6A, the plasma concentration of curcumin was higher in animals treated with nanotized curcumin as compared to those receiving native curcumin. The pharmacokinetics parameters are listed in Table 1. Notably, the  $C_{max}$  of nanotized curcumin was observed to be increased by almost 20-fold in comparison to native curcumin. The  $AUC_{0-\infty}$  of nanotized curcumin was increased by eleven-fold in comparison to native curcumin, demonstrating that the nanotized curcumin formulation was able to improve the oral BA of curcumin. The  $K_{el}$  of nanotized curcumin were also increased by four-fold over that of native curcumin (Table 1).

## Dose determination of native and nanotized curcumin for treating experimental cerebral malaria in C57BL/6 mice

C57BL/6 mice were infected with blood-stage *P. berghei*-ANKA as discussed in the experimental section. After 24 hours of infection, mice were orally treated with various doses of curcumin and its nanotized counterpart. It was observed that all control mice developed hypothermia by day 2, ataxia and convulsions by day 3, and died by day 8; whereas the treated groups had considerably higher longevity (32–34 days; Figure 6B). Mice treated with 20 mg/kg body weight and 40 mg/kg body weight of nanotized curcumin showed the longest survival (34 days), whereas mice treated with the same dose of native curcumin showed survival to 22 days (Figure 6B). Likewise, mice treated with 10 mg/kg body weight of the nanotized and native forms of curcumin survived to days 30 and 20, respectively. Though each group

of malaria-infected animals developed hypothermia by day 4, convulsions and ataxia development were delayed in the case of mice treated with nanotized curcumin. The longevity of malaria-infected mice was further extended to more than 2 months upon increasing the treatment schedule with nanoencapsulated nifetepimine for 1 month. Peterson's test indicated a reduction in the parasitemia levels after day 6, which approached a nearly undetectable level by day 15 in the *P. berghei*-infected group of mice treated with nanotized curcumin (Figure 6C and D). Thus, treatment with nanotized curcumin significantly delayed the onset of hypothermia and prevented convulsions, ataxia, paralysis, etc, which are the vital symptoms associated with cerebral malaria.

## Liver and kidney function tests

Elevated levels of alkaline phosphatase (ALP) and bilirubin are an indication of hepatocyte damage during malarial infection. Acute renal failure and increased levels of creatinine and urea have been also associated with severe forms of malaria. The ALP enzyme activity in the sera of normal mice was recorded to be  $7.28 \pm 0.72$  KA (Table 2). It increased significantly in the infected mice ( $39.43 \pm 3.82$  KA) by day 6, which was five times the normal value. A significant decrease in ALP activity was observed in the infected group of mice treated with nanotized curcumin by day 15 ( $12.12 \pm 1.36$  KA), followed by a more significant reduction by day 21 ( $7.90 \pm 0.63$  KA). Infected groups treated with native curcumin showed a less remarkable reduction in ALP values (Table 2). Serum bilirubin level was also found to be increased in the infected, untreated group of mice ( $2.61 \pm 0.45$  mg/dL) as compared to that in the infected group ( $1.41 \pm 0.16$  mg/dL) treated with nanotized curcumin on day 6. It was substantially reduced by day 15 and day 21 to 1.11 and 0.66 mg/dL, respectively. In comparison, the changes in serum bilirubin levels were moderately reduced to 1.6 and 2.10 mg/dL on day 6 and day 21, respectively, for the group treated with native curcumin (Table 2). Serum glutamate oxaloacetate transaminase (SGOT) activity was found to be  $12.45 \pm 0.63$  U/L in the normal group while in the infected group it was increased more than six times, ie,  $81.52 \pm 0.72$  U/L on day 6. Serum glutamate pyruvate transaminase (SGPT) was found to have five times more activity in infected untreated mice ( $146.22 \pm 2.76$  U/L) and native curcumin-treated ( $98.34 \pm 4.68$  U/L) mice on day 6. However, SGPT values were significantly reduced in infected groups of mice treated with nanotized curcumin by day 15 ( $75.46$  U/L) and day 21 ( $30.43 \pm 3.31$  U/L). In the normal group, the level of serum urea was determined to be  $31.23 \pm 2.3$  mg/dL, which

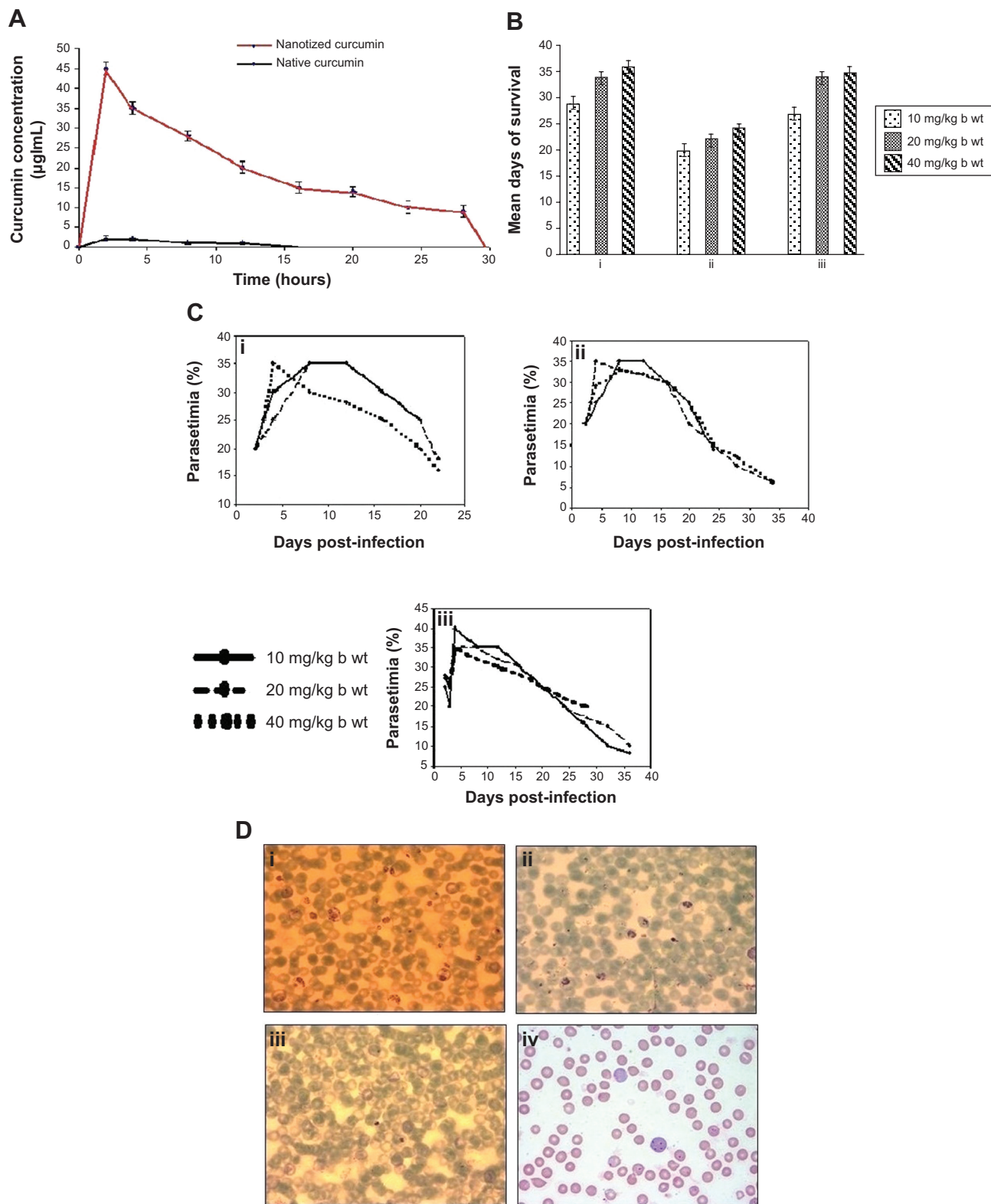


**Figure 6** (A) Plasma concentrations of native curcumin and nanotized curcumin after treatment with both the drugs. (B) Dose kinetics of (i) native curcumin, (ii) nanotized curcumin, and (iii) chloroquine at doses of 10, 20, and 40 mg/kg body weight administered orally to *Plasmodium berghei*-infected mice. Average number of days of survival (y-axis) was plotted against the respective dose. (C) Percentage parasitemia (y-axis) was plotted against mean days of survival (x-axis) of malaria-infected mice treated with 10, 20, and 40 mg/kg body weight of (i) native curcumin, (ii) nanotized curcumin, and (iii) chloroquine (positive control drug). (D) Parasitemia in *P. Berghei*-infected mice after 15 days of oral administration of (i) normal saline, (ii) native curcumin, and (iii) nanotized curcumin, respectively at a dose of 20 mg/kg body weight. (iv) Chloroquine was used as the control drug.

**Note:** Data are presented as mean ± standard error of the mean (n=6).  
**Abbreviation:** b wt, body weight.

**Table 1** Pharmacokinetics parameters of native and nanotized curcumin after oral administration

Compound formulations	Dose (mg/kg)	C <sub>max</sub> (µg/mL)	T <sub>max</sub> (h)	K <sub>el</sub> (h <sup>-1</sup> )	AUC <sub>0-∞</sub> µg/mL/min	Relative BA
Native curcumin in DMSO	40	0.452±0.31	1	0.031	16.7	
Nanotized curcumin in water	40	9.231±2.21	4	0.142	210.54	9.5

**Note:** Data for C<sub>max</sub> are presented as mean ± SEM (n=6).

**Abbreviations:** AUC, area under the curve; BA, bioavailability; C<sub>max</sub>, maximum concentration; DMSO, dimethyl sulfoxide; K<sub>el</sub>, elimination rate constant; T<sub>max</sub>, time at C<sub>max</sub>; SEM, standard error of the mean.

increased by more than two-fold (76.54±2.81 mg/dL) in the infected group of mice on day 6. Upon prolonged treatment with nanotized curcumin, there was a sharp decrease in the concentration of urea (48.34±3.04 mg/dL) in the infected group of mice by day 6, approaching that of the normal, uninfected group (Table 2). Increased creatinine concentration, indicative of renal disorders, was evident in the infected untreated group (4.39±0.24 mg/dL), and native curcumin-treated infected group (4.29±0.37 mg/dL) as compared to that of normal mice (1.15±0.22 mg/dL) by day 6. The concentration of creatinine in infected groups of animals treated with nanotized curcumin was found to be 2.30 mg/dL by day 6 and the level nearly reached the normal value by day 21 (1.18 mg/dL) as shown in Table 2.

This observation suggests that efficient disposal of parasites by nanotized curcumin (Figure 6D) ameliorates liver damage, highlighting its reversible nature during *P. Berghei*-ANKA infection.

## Discussion

Development of resistance against multiple drugs and non-specific targeting of intracellular parasites require high doses

and subsequent toxicity has remained the major drawback of conventional malaria chemotherapy. New strategies for intracellular antimalarial delivery need to be developed in order to prevent drug-resistance mechanisms in malaria therapy. The main purpose of malaria therapy is to maintain a high drug concentration in the intracellular parasitophorous vacuole where the *Plasmodium* is located in the RBCs.<sup>9</sup>

Curcuminoids, isolated from the rhizome of *C. longa*, have been in use for several centuries as therapeutic and health-promoting agents. Curcuminoids have a series of biological activities such as antitumor, antioxidant, anti-amyloid, antiinflammatory, hypocholesteremic, and anti-HIV properties.<sup>27,28</sup> Recently, curcuminoids were reported to have antimalarial activity in both in vitro (chloroquine-resistant and -sensitive *P. falciparum* lab strains) and in vivo (*P. berghei*) studies.<sup>27,28</sup> Studies carried out both in vitro and in vivo also indicated that curcumin possesses moderate antimalarial activity with an IC<sub>50</sub> ranging 5–10 µM in vitro.<sup>9</sup> When administered orally for five consecutive days, curcumin reduces the parasite burden by more than 80% and protects up to 29% of *P. berghei*-infected mice.<sup>9</sup> However, its poor water solubility at physiological pH, limited absorption,

**Table 2** Liver and kidney function tests of the normal, infected (untreated) control, and chloroquine-, native curcumin-, and nanocurcumin-treated groups of mice

Groups	Day of the measurement	ALP (KA units)	Bilirubin (mg/dL)	SGOT activity (U/L)	SGPT activity (U/L)	Urea (mg/dL)	Creatinine (mg/dL)	
Normal mice	6	7.28±0.72	0.57±0.12	12.45±0.63	27.20±1.34	31.23±2.32	1.15±0.12	
	15	8.16±0.54	0.61±0.14	13.32±0.51	28.24±1.62	32.50±2.45	1.25±0.21	
	21	8.13±0.47	0.59±0.16	13.21±0.66	28.13±1.52	31.82±2.34	1.21±0.23	
Infected control (A)	6	39.43±3.82	2.61±0.45	81.52±0.72	146.22±2.76	76.54±4.81	4.39±0.24	
	(A) + chloroquine treated	6	16.4±2.61	1.15±0.16	36.20±0.72	39.41±4.32	50.32±2.43	2.10±0.24
		15	10.6±2.31	1.82±0.18	33.31±0.61	32.34±3.42	40.82±2.51	1.60±0.27
(A) + native curcumin treated	6	7.21±2.41	0.60±0.24	14.14±0.51	30.17±3.61	33.44±2.56	1.23±0.17	
	15	30.72±2.92	1.60±0.36	66.43±0.65	98.34±4.68	54.24±2.37	3.29±0.37	
	21	28.81±2.65	2.19±0.20	72.80±0.71	102.69±5.71	61.72±2.61	2.90±0.46	
(A) + nanocurcumin treated	6	36.91±2.67	2.10±0.25	75.71±0.47	136.31±6.45	87.46±2.54	2.70±0.51	
	15	18.33±1.41	1.41±0.16	45.40±4.12	75.46±4.26	48.34±3.04	2.30±0.21	
	21	12.12±1.36	1.11±0.21	24.28±3.72	50.31±3.69	41.62±3.21	2.14±0.23	
	21	7.90±0.63	0.66±0.06	13.45±3.25	30.43±3.31	32.36±3.16	1.18±0.51	

**Note:** Values are mean ± SEM (n=6).

**Abbreviations:** ALP, alkaline phosphatase; SEM, standard error of the mean; SGOT, serum glutamate oxaloacetate transaminase; SGPT, serum glutamate pyruvate transaminase.

poor BA, and chemical instability are major concerns for increasing its efficacy.

Biodegradable nanoparticles have been developed for intracellular drug delivery, especially for drugs with an intracellular target, which bear potential as antimalarials.<sup>29</sup> The most beneficial property of nanoparticles in treating malaria is their ability to improve the interaction with infected RBCs and parasite membranes.<sup>30</sup> A group of researchers have also suggested that antimalarial nanocarriers (<80 nm) may access parasitic intracellular compartments through membrane channels called “new permeability pathways” that appear after *Plasmodium* invasion in RBCs.<sup>31</sup>

Numerous attempts have been made to increase the therapeutic efficiency of curcuminoids using lipid and polymeric nanoparticles. These attempts succeeded to a certain extent; however, some drawbacks associated with these formulations include difficulty in large-scale manufacturing, high cost of excipients in the case of liposomes, insufficient lipid carrier in the case of solid lipid nanoparticles, and long-term stability in the case of emulsions.<sup>32</sup> On the other hand, the method reported here for the preparation of nanotized curcumin is easily scalable.

The purpose of using nanotized formulations is to improve solubility and target selectivity, to reduce the frequency of administration and the duration of the treatment, and to improve the pharmacokinetic profile of the drug. In the present study, chemically synthesized curcumin was used to formulate nanotized curcumin, which is independent of any polymeric or lipidic nanocarrier. Interestingly, the particle size range of the nanotized curcumin described in the study was found to be within 20–50 nm from TEM, AFM, and DLS studies (Figure 1). Moreover, it was observed that nanotized curcumin was readily dispersible in water in comparison to its native counterpart, which was found to be completely insoluble in water (Figure 1). The increased aqueous dispersibility of nanotized curcumin particles could be accredited to their larger surface area, which promotes homogeneous dispersion.<sup>33</sup> It has been well-documented<sup>34</sup> in several previous studies that particle size reduction of active compounds to nanoparticulate form leads to improvement in their dispersibility, efficacy, solubility, and BA. The particle charge is one of the factors determining the physical stability of emulsions and suspensions. The more particles that bear the same charge, the greater the electrostatic repulsion between those particles, thus lending higher physical stability due to reduced likelihood of aggregation. In the present study, the zeta potential value of nanotized curcumin was found to be  $63.2 \pm 6.96$  mV (Figure 1), suggesting higher stability of the

particles.<sup>34</sup> FT-IR studies were conducted further to make sure that the curcumin is present in its nanoform and that there was no structural change (Figure 2A). Moreover, the loading and encapsulation efficiency of nanotized curcumin was found to be 4.25% and 45%, respectively. It is evident that the presence of DMAB played a predominant role in the nanotization of curcumin, with more entrapment efficiency. It could therefore be suggested that DMAB's positive charge may have been the cause of this high encapsulation efficiency.

The physicochemical properties of free and nanotized curcumin were evaluated using DTA. The data provided qualitative information about the physical state of curcumin present in the nanoformulation (Figure 2B). The DTA thermogram of DMAB, free curcumin, and its nanoformulation showed that their glass transition (main phase transition) temperature peaked between 70°C and 80°C. The DTA thermogram of free curcumin showed an intense endothermic peak at 177°C that corresponded to the melting temperature of curcumin crystal. In the nanoformulation, the prominent melting peak of curcumin at 177°C disappeared, while the glass transition temperature of nanotized curcumin existed between 70°C–80°C, at which the curcumin molecules were completely entrapped, included, and covered by polymeric chains of DMAB. The absence of the crystalline nature of curcumin in the nanoformulation was due to a complete coverage of the drug by the polymeric chains of DMAB.

Figure 3A shows the release profiles of curcumin from the nanotized formulation in PBS medium. Around 50% of the curcumin was released from the nanotized formulation after 24 hours, followed by a sustained release until 48 hours. Moreover, around 10% of the drug was retained by the nanotized formulation, suggesting robust encapsulation of curcumin within the nanotized formulation. This was further emphasized by the observed change in fluorescence intensity of nanotized curcumin when compared with that of native curcumin (350 au vs 200 au) (Figure 3B), suggesting high entrapment efficiency of nanotized curcumin.

These characterization studies showed that the nanoformulation of curcumin had better bioefficacy compared to that of its native counterpart and had no associated toxicity as observed with polymeric or lipidic nanocarriers (Figure 4). Although enhancement in the cytotoxicity of curcumin-loaded polymer nanoparticles has been reported previously,<sup>35</sup> the described nanotized curcumin in the present study was not prepared with any synthetic polymers, which themselves can be toxic to cellular systems. Consequently,



the nanoformulation described here may offer an added advantage of high biocompatibility with low or no cellular toxicity. We also found that nanotized curcumin had much higher cellular uptake in vitro as compared to its native counterpart (Figure 5A). The preparation was found to be highly effective in reducing blood-stage parasitemia and had an  $IC_{50}$  value of 0.5  $\mu$ M compared to 5  $\mu$ M for native curcumin (Figure 5B and C).

Studies conducted by a group have shown that the attributes of nanoformulations, such as greater surface area for dissolution and absorption; quick onset of action; increased saturation solubility of the drug;<sup>36</sup> and increased adhesiveness of nanoformulations to gastrointestinal mucosa, result in improved oral BA and reduced pharmacokinetic variability of hydrophobic compounds such as curcumin. In vivo pharmacokinetic analysis in the present study showed that the oral BA of nanotized curcumin increased significantly compared to that of native curcumin (Figure 6A). The increased oral BA of nanotized curcumin may largely be attributed to the increase in its aqueous dispersion. As shown in Table 1, upon oral treatment with native curcumin at a dose of 40 mg/kg body weight in mice, the  $C_{max}$  could be detected in the blood at 1 hour post-feeding. In contrast, when the same amount of nanotized curcumin was fed to another group of mice, the  $C_{max}$  was detected in the blood at 4 hours.

The concentration of curcumin detected in the blood plasma was significantly higher in mice fed with nanotized curcumin than those administered with an equimolar concentration of native curcumin at all time-points studied (Figure 6A). Oral delivery of nanotized curcumin ensured a sustained release of curcumin until 30 hours post-feeding, whereas in the case of treatment with native curcumin, the levels declined significantly after 10 hours and were not detectable beyond 15 hours. The positive surface charge of DMAB provided a means to aid drug adsorption and delivery, since it is expected to ensure better interaction with the negatively charged cell membranes.<sup>37</sup> This may result in an increased retention time at the cell surface, thus increasing the chances of particle uptake and improving drug BA.<sup>38</sup>

In vivo antimalarial efficacy of native and nanotized curcumin in *P. berghei*-infected mice is presented in Figure 6. Upon oral treatment with the nanotized formulation, mice infected with blood-stage *P. berghei*-ANKA survived for 34 days (Figure 6B), with almost complete clearance of the parasites (Figure 6C and D), whereas those treated with only native curcumin survived for 22 days (Figure 6B). Moreover, when the treatment schedule with nanotized curcumin was

prolonged for 1 month more, the malaria-infected mice survived for more than 2 months with a gradual reduction in parasitemia and almost 50% of the animals achieved ultimate cure. The onset of pathological symptoms like ataxia, convulsions, and hypothermia was also delayed in the nanotized curcumin-treated group as compared to the native curcumin-treated group. Therefore, a considerable increase in the lifespan of the mice treated with nanotized curcumin was observed in comparison to the native curcumin-treated mice.

The increased serum ALP, SGOT, and SGPT activities were observed due to compromised liver function during malarial infection in mice.<sup>39–42</sup> Serum bilirubin concentration (>3 mg/dL) is a common feature accredited to liver damage and hemolysis of parasitized and non-parasitized cells.<sup>40</sup> In nanotized curcumin-treated malaria-infected mice, ALP, SGOT, and SGPT activities, as well as bilirubin levels were reduced in the serum to almost normal levels (Table 2), a response similar to that evoked when treated with chloroquine. In the infected untreated group, bilirubin concentration increased four-fold as compared to that in normal mice, thereby indicating jaundice-like symptoms (Table 2). Native curcumin, on the other hand, offered only minor protection.

Serum urea and creatinine concentration are used for renal sufficiency assessment.<sup>42–44</sup> Serum urea and creatinine levels were recorded to be significantly increased in the infected control as compared to the normal group of mice. Higher levels of serum urea and creatinine are indications of deficiency in renal function.<sup>44,45</sup> Unlike its native counterpart, treatment with nanotized curcumin lead to a reduction in serum urea and creatinine levels (Table 2), imparting significant protection to the kidneys of infected groups of mice. This protective effect of nanotized curcumin was very similar to that of chloroquine.

Moreover, curcumin generates reactive oxygen species and thereby specifically inhibits PfGCN5 HAT activity in *P. falciparum*.<sup>46</sup> Therefore, like its native counterpart, nanotized curcumin-induced generation of reactive oxygen species may lead to more efficacious histone hypoacetylation and DNA damage that ultimately could account for the parasitocidal effect of nanotized curcumin.

In summary, using a murine model of malaria as a prototype protozoal disease, we demonstrate the striking therapeutic potential of nanotized curcumin, delivered orally, for treating malaria. Adaptation of this nanotization approach holds considerable promise for harnessing the therapeutic potential of a number of well-tolerated natural molecules.

## Acknowledgments

AS is a Bhatnagar Fellow of the Council of Scientific and Industrial Research (CSIR), India. This work is supported by a grant from CSIR. The authors thank Professor William J Wehlan (Fellow of the Royal Society, Department of Biochemistry and Molecular Biology, Miller School of Medicine, University of Miami, FL, USA), for reading the manuscript. The authors thank Mr ATM Muruganandan (Technical Officer, Indian Institute of Chemical Biology [IICB], Kolkata, India), for his contribution in operating the AFM and Dr Aparna Lashkar (Technical Officer, IICB, Kolkata, India), for TEM operation, Mrs Ujwala Das (Technical Officer, Indian Association for Cultivation of Science), for zeta potential studies, and Mr Pranab De (Technical Officer, Bose Institute, Kolkata, India) for DLS operation. The authors wish to thank Dr Nirmalendu Das (IICB, Kolkata, India), Dr Krishna Das Saha (IICB, Kolkata, India), Debasree Ghosh (IICB, Kolkata, India), Dr Biswajoy Bagchi (Jadavpur University, Kolkata, India), and Professor Parimal C Sen (Bose Institute, Kolkata, India) for their help and support during the work. Authors also wish to thank Chandresh Bhagatani for general assistance.

## Disclosure

The authors report no conflicts of interest in this work.

## References

- Calabrese V, Bates TE, Mancuso C, et al. Curcumin and the cellular stress response in free radical-related diseases. *Mol Nutr Food Res*. 2008;52(9):1062–1073.
- Motterlini R, Foresti R, Bassi R, Green CJ. Curcumin, an antioxidant and anti-inflammatory agent, induces heme oxygenase-1 and protects endothelial cells against oxidative stress. *Free Radic Biol Med*. 2000;28(8):1303–1312.
- Goel A, Kunnumakkara AB, Aggarwal BB. Curcumin as “Curecumin”: from kitchen to clinic. *Biochem Pharmacol*. 2008;75(4):787–809.
- Adapalal N, Chan MM. Long-term use of an anti-inflammatory, curcumin, suppressed type 1 immunity and exacerbated visceral leishmaniasis in a chronic experimental model. *Lab Invest*. 2008;88(12):1329–1339.
- Nose M, Koide T, Ogihara Y, Yabu Y, Ohta N. Trypanocidal effects of curcumin in vitro. *Biol Pharm Bull*. 1998;21(6):643–645.
- Pérez-Arriaga L, Mendoza-Magaña ML, Cortés-Zárate R, et al. Cytotoxic effect of curcumin on *Giardia lamblia* trophozoites. *Acta Trop*. 2006;98(2):152–161.
- Cui L, Miao J, Cui L. Cytotoxic effect of curcumin on malaria parasite *Plasmodium falciparum*: inhibition of histone acetylation and generation of reactive oxygen species. *Antimicrob Agents Chemother*. 2007;51(2):488–494.
- Nandakumar DN, Nagaraj VA, Vathsala PG, Rangarajan P, Padmanaban G. Curcumin-artemisinin combination therapy for malaria. *Antimicrob Agents Chemother*. 2006;50(5):1859–1860.
- Reddy RC, Vatsala PG, Keshamouni VG, Padmanaban G, Rangarajan PN. Curcumin for malaria therapy. *Biochem Biophys Res Commun*. 2005;326(2):472–474.
- Ringman JM, Frautschy SA, Cole GM, Masterman DL, Cummings JL. A potential role of the curry spice curcumin in Alzheimer’s disease. *Curr Alzheimer Res*. 2005;2(2):131–136.
- Barratt GM. Colloidal drug carriers: achievements and perspectives. *Cell Mol Life Sci*. 2003;60(1):21–37.
- Forrest ML, Kwon GS. Clinical developments in drug delivery nanotechnology. *Adv Drug Deliv Rev*. 2008;60(8):861–862.
- Murthy SK. Nanoparticles in modern medicine: state of the art and future challenges. *Int J Nanomedicine*. 2007;2(2):129–141.
- Bisht S, Feldmann G, Soni S, et al. Polymeric nanoparticle-encapsulated curcumin (“nanocurcumin”): a novel strategy for human cancer therapy. *J Nanobiotechnology*. 2007;5:3.
- World Health Organization. Severe falciparum malaria. World Health Organization, Communicable Diseases Cluster. *Trans R Soc Trop Med Hyg*. 2000;94 Suppl 1:S1–S90.
- Rest JR. Cerebral malaria in inbred mice. I. A new model and its pathology. *Trans R Soc Trop Med Hyg*. 1982;76(3):410–415.
- Pabon HJ. A synthesis of curcumin and related compounds. *Recl Trav Chim Pays Bas*. 1964;83(4):379–386.
- Hariharan S, Bhardwaj V, Bala I, Sitterberg J, Bakowsky U, Ravi Kumar MN. Design of estradiol loaded PLGA nanoparticulate formulations: a potential oral delivery system for hormone therapy. *Pharm Res*. 2006;23(1):184–195.
- Ghosh A, Sarkar S, Mandal AK, Das N. Neuroprotective role of nanoencapsulated quercetin in combating ischemia-reperfusion induced neuronal damage in young and aged rats. *PLoS One*. 2013; 8(4):e57735.
- Changtam C, de Koning HP, Ibrahim H, Sajid MS, Gould MK, Suksamrarn A. Curcuminoid analogs with potent activity against *Trypanosoma* and *Leishmania* species. *Eur J Med Chem*. 2010; 45(3):941–956.
- Ruozzi B, Tosi G, Leo E, Vandelli MA. Application of atomic force microscopy to characterize liposomes as drug and gene carriers. *Talanta*. 2007;73(1):12–22.
- Sahu A, Bora U, Kasoju N, Goswami P. Synthesis of novel biodegradable and self-assembling methoxy poly(ethylene glycol)-palmitate nanocarrier for curcumin delivery to cancer cells. *Acta Biomater*. 2008;4(6):1752–1761.
- Mosmann T. Rapid colorimetric assay for cellular growth and survival: application to proliferation and cytotoxicity assays. *J Immunol Methods*. 1983;65(1–2):55–63.
- Tønnesen HH, Kristensen S, Grinberg LN. Studies on curcumin and curcuminoids: XXV. Inhibition of primaquine-induced lysis of human red blood cells by curcumin. *Int J Pharm*. 1994;110(2):161–167.
- Houwen B. Blood film preparation and staining procedures. *Clin Lab Med*. 2002;22(1):1–14.
- Peterson I, Wroblewski JS. Mortality rates of fishes in the pelagic ecosystem. *Can J Fish Aquat Sci*. 1984;41(7):1117–1120.
- Larisa N, David D, Donna MP. Chemopreventive anti-inflammatory activities of curcumin and other phytochemicals mediated by MAP kinase phosphatase-5 in prostate cells. *Carcinogenesis*. 2007;28(6):1188–1196.
- Gandapu U, Chaitanya RK, Kishore G, Reddy RC, Kondapi AK. Curcumin-loaded apotransferrin nanoparticles provide efficient cellular uptake and effectively inhibit HIV-1 replication in vitro. *PLoS One*. 2011;6(8):e23388.
- Santos-Magalhães NS, Mosqueira VC. Nanotechnology applied to the treatment of malaria. *Adv Drug Deliv Rev*. 2010;62(4–5):560–575.
- Anand P, Kunnumakkara AB, Newman RA, Aggarwal BB. Bioavailability of curcumin: problems and promises. *Mol Pharmaceutics*. 2007;4(6):807–818.
- Kakkar V, Singh S, Singla D, Kaur IP. Exploring solid lipid nanoparticles to enhance the oral bioavailability of curcumin. *Mol Nutr Food Res*. 2011;55(3):495–503.
- Kirk K, Saliba KJ. Targeting nutrient uptake mechanisms in *Plasmodium*. *Curr Drug Targets*. 2007;8(1):75–88.
- Nair KL, Thulasidasan AK, Deepa G, Anto RJ, Kumar GS. Purely aqueous PLGA nanoparticulate formulations of curcumin exhibit enhanced anticancer activity with dependence on the combination of the carrier. *Int J Pharm*. 2012;425(1–2):44–52.

34. Balavandy SK, Shamel K, Biak DR, Abidin ZZ. Stirring time effect of silver nanoparticles prepared in glutathione mediated by green method. *Chem Cent J*. 2014;8(1):11.
35. Tiyaaboonchai W, Tungpradit W, Plianbangchang P. Formulation and characterization of curcuminoids loaded solid lipid nanoparticles. *Int J Pharm*. 2007;337(1-2):299-306.
36. Kang MJ, Cho JY, Shim BH, Kim DK, Lee J. Bioavailability enhancing activities of natural compounds from medicinal plant. *J Med Plants Res*. 2009;3(13):1204-1211.
37. Song C, Labhasetwar V, Cui X, Underwood T, Levy RJ. Arterial uptake of biodegradable nanoparticles for intravascular local drug delivery: results with an acute dog model. *J Control Release*. 1998;54(2):201-211.
38. Bhardwaj V, Ankola DD, Gupta SC, Schneider M, Lehr CM, Kumar MN. PLGA nanoparticles stabilized with cationic surfactant: safety studies and application in oral delivery of paclitaxel to treat chemical-induced breast cancer in rat. *Pharm Res*. 2009;26(11):2495-2503.
39. Garba IH, Ubom G. Serum alkaline phosphatase activity as a potential biomarker for the integrity of the hepatic drainage system in acute falciparum malaria infection. *Int J Infect Dis*. 2005;4(2):2.
40. Wilairatana P, Looareesuwan S, Charoenlarp P. Liver profile changes and complications in jaundiced patients with falciparum malaria. *Trop Med Parasitol*. 1994;45(4):298-302.
41. Wroblewski F, La Due JS. Serum glutamic oxaloacetic transaminase activity as an index of liver cell injury from cancer; a preliminary report. *Cancer*. 1955;8(6):1155-1163.
42. Molander DW, Sheppard E, Payne MA. Serum transaminase in liver disease. *J Am Med Assoc*. 1957;163(16):1461-1465.
43. Smith GL, Shlipak MG, Havranek EP, Foody JM, Masoudi FA. Serum urea, nitrogen, creatinine and estimators of renal function. *Arch Int Med*. 2006;166(10):1134-1142.
44. Narayanan S, Appleton HD. Creatinine: a review. *Clin Chem*. 1980;26(8):1119-1126.
45. Mouton R, Holder K. Laboratory tests of renal function. *Anaes Int Care Med*. 2006;7(7):240-243.
46. Joe B, Vijaykumar M, Lokesh BR. Biological properties of curcumin-cellular and molecular mechanisms of action. *Crit Rev Food Sci Nutr*. 2004;44(2):97-111.

### International Journal of Nanomedicine

## Publish your work in this journal

The International Journal of Nanomedicine is an international, peer-reviewed journal focusing on the application of nanotechnology in diagnostics, therapeutics, and drug delivery systems throughout the biomedical field. This journal is indexed on PubMed Central, MedLine, CAS, SciSearch®, Current Contents®/Clinical Medicine,

Submit your manuscript here: <http://www.dovepress.com/international-journal-of-nanomedicine-journal>

Dovepress

Journal Citation Reports/Science Edition, EMBase, Scopus and the Elsevier Bibliographic databases. The manuscript management system is completely online and includes a very quick and fair peer-review system, which is all easy to use. Visit <http://www.dovepress.com/testimonials.php> to read real quotes from published authors.